



Cite this: *Chem. Commun.*, 2016, 52, 4545

Received 20th December 2015,  
Accepted 29th February 2016

DOI: 10.1039/c5cc10440h

www.rsc.org/chemcomm

## Photoactivatable CO release from engineered protein crystals to modulate NF- $\kappa$ B activation†

Hiroyasu Tabe,<sup>a</sup> Takuya Shimoi,<sup>b</sup> Marion Boudes,<sup>c</sup> Satoshi Abe,<sup>b</sup> Fasséli Coulibaly,<sup>c</sup> Susumu Kitagawa,<sup>\*a</sup> Hajime Mori<sup>d</sup> and Takafumi Ueno<sup>\*b</sup>

**Photoactivatable CO releasing protein crystals were developed by immobilization of Mn carbonyl complexes in polyhedral crystals, which are spontaneously formed in insect cells. The photoactivatable CO release from the engineered protein crystals activates nuclear factor kappa B (NF- $\kappa$ B) upon stimulation by visible light irradiation with suppression of cytotoxicity of the Mn complex.**

Carbon monoxide (CO) is one of several gaseous cellular-signaling molecules operating in living cells. CO mediates anti-inflammation and vasoactive response, and has been used to control immune responses during transplantation.<sup>1,2</sup> CO signaling involves interactions with other gaseous signaling molecules such as nitric oxide and hydrogen sulfide, which are endogenously produced by the specific enzymes.<sup>3,4</sup> Recently, the therapeutic applications of CO have attracted significant attention as a result of rapid development of a number of CO-releasing molecules (CORMs).<sup>5</sup> Metal carbonyl complexes such as [Ru(CO)<sub>3</sub>Cl<sub>2</sub>]<sub>2</sub> (CORM-2) and Ru(CO)<sub>3</sub>Cl(glycinate) (CORM-3), have been used to deliver CO into living cells.<sup>6</sup> Synthetic and natural carrier molecules have been developed with the objective of providing safe and controlled delivery of CORMs into cells, tissues, and animals with effective CO-releasing properties.<sup>7–13</sup> Moreover, a wide variety of transition metals and synthetic ligands have been developed for stimulus-induced CO release.<sup>14–16</sup> These efforts represent promising strategies for providing controlled CO delivery.

Photoactivation is one of the most favorable external stimuli for CORMs. Other external stimuli include pH change, and enzymatic reactions.<sup>14–16</sup> Photoactivatable CORMs (photoCORMs) are transition metal carbonyl complexes of Mn,<sup>17–19</sup> Fe,<sup>20–22</sup> Ru,<sup>23</sup> and Re,<sup>18,24</sup> among others. Since Motterlini *et al.* reported that Mn<sub>2</sub>(CO)<sub>10</sub> (CORM-1) can release CO with triggering by light irradiation,<sup>25</sup> design of photoCORMs has been achieved by development of complexes based on organic ligands coordinating to Mn ions.<sup>17–19</sup> Recently, Mascharak and co-workers have reported photoCORMs of Mn carbonyl complexes with polypyridine-based ligands to promote rapid CO release in the visible/near infrared region.<sup>26</sup> For biotechnological applications of photoCORMs, cytotoxicity arising from free metal ions, organic ligands, or by the reaction of photoCORMs with light irradiation should be considered.<sup>27,28</sup> One of the possible solutions is provided by incorporation of photoCORMs into biocompatible scaffolds to prevent release of metal ions or synthetic organic ligands.<sup>26</sup> Nanoparticles, polymers, and porous materials have been utilized as molecular matrices for stable accumulation of photoCORMs.<sup>8,11,26,29,30</sup> Schatzschneider and co-workers have utilized silica nanoparticles as photoCORM carriers.<sup>11</sup> [Mn(CO)<sub>3</sub>(pqa)]ClO<sub>4</sub> incorporated into Al-MCM-41 nanoparticles were found to promote vasorelaxation of rat aorta muscle rings through light-induced CO delivery.<sup>26</sup> PhotoCORMs have been non-covalently and covalently embedded into polymers.<sup>30</sup> However, their CO releasing properties have slow rates of *ca.* 20 min. Thus, improvement of carrier matrices for photoCORMs is required for design of photoCORMs with rapid responses to stimuli.

It has been recently reported that proteins and protein assemblies can serve as biocompatible carriers of CORMs.<sup>31–37</sup> Composites of protein assemblies with CORMs can stably deliver CO into living cells and effectively release them to activate signal transduction.<sup>33–37</sup> Protein crystals are also expected to be appropriate candidates for extracellular matrices (ECMs) for immobilization of CORMs because protein crystals represent precise protein assemblies in the solid state with inner pores that act as “solvent channels.”<sup>33,34</sup> In general, when most of the crystals are

<sup>a</sup> Graduate School of Engineering, Kyoto University, Katsura, Nishikyo-ku, Kyoto 615-8510, Japan. E-mail: kitagawa@icems.kyoto-u.ac.jp

<sup>b</sup> Graduate School of Bioscience and Biotechnology, Tokyo Institute of Technology, Nagatsuta 4259, Midori-ku, Yokohama 224-8501, Japan. E-mail: tueno@bio.titech.ac.jp

<sup>c</sup> Infection and Immunity Program, Monash Biomedicine Discovery Institute and Department of Biochemistry and Molecular Biology, Monash University, Melbourne, VIC3800, Australia

<sup>d</sup> Insect Biomedical Research Center, Kyoto Institute of Technology, Matsugasaki, Sakyo-ku, Kyoto 606-8585, Japan

† Electronic supplementary information (ESI) available: Details of experiments, structures and crystallographic dates; Fig. S1–S4; Tables S1. See DOI: 10.1039/c5cc10440h



stabilized by cross-linking, the crystals are utilized as vessels for preparation of metal nanoparticles or catalytic reactions by immobilization of metal compounds under various reaction conditions.<sup>38</sup> It has been reported that cross-linked hen egg white lysozyme crystals can serve as extracellular matrices for CORM-2.<sup>33</sup> However, inconvenient procedures which include crystallization and cross-linking are required to obtain the materials. To address this issue, we have used protein crystals, which are spontaneously synthesized in insect cells, as matrices for immobilizing CORMs.<sup>34</sup> Polyhedral crystals (PhCs) are directly produced from polyhedrin monomer (PhM) expressed in insect cells after infection by cypovirus.<sup>39</sup> PhCs are highly stable over a wide range of pH, temperature, and in organic solvents, and can be frozen or dried because their original function is to provide protective material to store replicated viruses produced during the viral infection cycle.<sup>39</sup> PhCs have served as extracellular matrices for growth factors and CORMs due to their biocompatibility.<sup>34,40</sup> In this article, we describe the immobilization of photoCORMs of Mn carbonyl complexes in PhCs, which can be used as ECM without cross-link treatment. To modulate the amounts of CO released from the composite, we increased the number of photoCORMs accumulated in PhCs by using a mutant of PhM with a hexa-histidine tag (His-tag) at its C-terminus (HTPhM). The crystal of HTPhM (HTPhC) containing Mn carbonyl complexes (**Mn-HTPhC**) has twice the number of Mn carbonyl complexes of WTPHC containing Mn carbonyl complexes (**Mn-WTPHC**). **Mn-HTPhC** was found to be capable of acting as an ECM that can release CO gas into living cells with a more rapid response than that of previously reported ECM-containing photoCORMs and activate nuclear factor kappa B (NF- $\kappa$ B) with visible light irradiation (Fig. 1).

HTPhCs were prepared as reported previously using an insect cell expression system of *Spodoptera frugiperda* 21 (Sf21).<sup>40</sup> To immobilize Mn(CO) moieties into HTPhCs, HTPhCs ( $7.8 \times 10^7$  crystals) were soaked in 10 mM HEPES buffer (pH 7.0, 500  $\mu$ L) containing 10% v/v acetonitrile and 1 mM Mn(CO)<sub>5</sub>Br. After gentle stirring for 24 hours at room temperature in the dark, the suspension was washed twice with Milli-Q water.

Fluorescence X-ray analysis of **Mn-HTPhC** showed that the number of Mn ions per HTPhM was  $5.6 \pm 1.2$ . The Mn

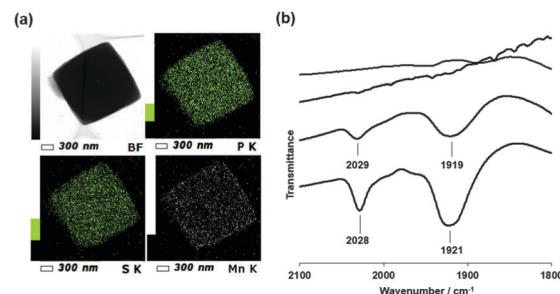


Fig. 2 STEM-EDX images of **Mn-HTPhC** (a): STEM bright-field (BF) image (upper left), elemental mapping images of P-K (upper right), S-K (bottom left) and Mn-K (bottom right). Infrared spectra (b): **Mn-HTPhC** (solid line), **Mn-WTPHC** (dashed line), **Mn-HTPhC** under the Mb assay conditions with visible light irradiation for 10 min (chained line), and HTPhC (dotted line). All the samples were measured as KBr pellets.

complexes were fully dispersed in **Mn-HTPhC** as confirmed by a scanning transmission electron microscopy-energy dispersive X-ray spectrum (STEM-EDX) (Fig. 2a). The IR spectrum of **Mn-HTPhC** has two bands at 1921 and 2028  $\text{cm}^{-1}$ . This set of bands is assigned to the CO stretching vibrations of the *fac*-Mn(CO)<sub>3</sub>(H<sub>2</sub>O)<sub>2</sub>(His) moiety.<sup>41</sup> **Mn-WTPHCs** were also prepared under the same conditions. The number of Mn per WTPHC in **Mn-WTPHC** ( $2.6 \pm 0.3$ ) was found to be almost half the value of that of **Mn-HTPhC** with homogeneously-dispersed accumulation (Fig. S1, ESI†). The IR spectrum of **Mn-WTPHC** indicates the presence of Mn carbonyl moieties with a coordination structure similar to that of **Mn-HTPhC** (Fig. 2b).

The crystal structure of **Mn-HTPhC** was determined at a resolution of 1.8 Å (ESI†). The structure has no electron density for the extended sequence after Gly245, the carboxy-terminal residue in the wild-type protein. Moreover, an anomalous difference map does not identify densities assignable to Mn atoms in the structure although fluorescence X-ray analysis and STEM-EDX indicate the presence of Mn atoms in the composite. There is no electron density accounting for the presence of Mn in the crystal structure of **Mn-WTPHC** at a 1.7 Å resolution. These results suggest that the His-tag and Mn moieties can be oriented in several directions at the conjugation sites, as observed previously for Ru complexes conjugated in protein crystals.<sup>33</sup>

The photoactivatable CO-releasing properties of **Mn-HTPhC** were evaluated using the myoglobin (Mb) assay (Fig. 3 and Fig. S3, ESI†).<sup>7,25</sup> The data processing steps correct for the uneven absorption of the CORM at the Q-bands in both deoxy-Mb and carbonmonoxy-Mb (MbCO) (Fig. 3a).<sup>25,42</sup> **Mn-HTPhC** ( $4.0 \times 10^5$  crystals with immobilized Mn ions determined by ICP-MS is  $6.6 \times 10^{-4}$   $\mu\text{mol}$ ) was dispersed in 1 mL of a PBS buffer (pH 7.4) containing deoxy-Mb (6.2  $\mu\text{M}$ ) and sodium dithionite (30 mM). The reaction was accompanied by light irradiation at 456 nm using a blue LED light (130 mW, 33.2  $\text{mW cm}^{-2}$ , Fig. S2, ESI†). The total released amount of CO per Mn of **Mn-HTPhC** with light irradiation was found to be  $2.9 \pm 0.4$ . Significantly less CO released from **Mn-HTPhC** was detected without irradiation (Fig. 3b). The amount of CO released is consistent with the coordination structure

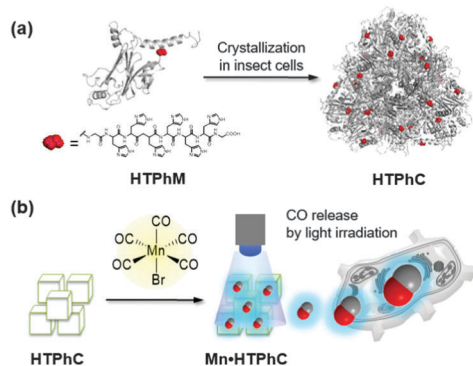
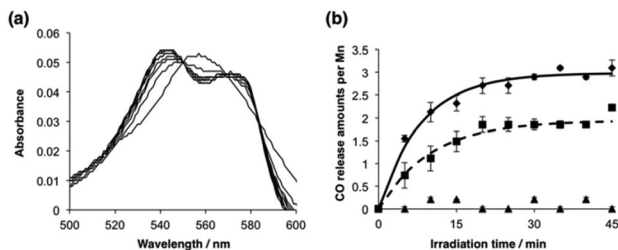


Fig. 1 Schematic drawings of polyhedrin monomer with a His-tag at the C terminus (HTPhM) to form crystal of HTPhMs (**HTPhC**) (a), and preparation of HTPhC containing Mn(CO)moieties (**Mn-HTPhC**) and CO release from Mn carbonyl moieties (b).





**Fig. 3** Mb assay of **Mn-HTPhC** and **Mn-WTPHC**: (a) time course of absorption spectral change of deoxy-Mb in a solution containing **Mn-HTPhC** with light irradiation, and (b) detection of CO release by plotting the concentration of MbCO. The absorption spectral change of MbCO was monitored for **Mn-HTPhC** with and without light irradiation (◆ and ▲, respectively), and **Mn-WTPHC** with light irradiation (■). All experiments were performed in 1 mL of 10 mM PBS buffer (pH 7.4) containing deoxy-Mb (6.2  $\mu$ M) and  $\text{Na}_2\text{S}_2\text{O}_4$  (30 mM). The Mn concentrations of **Mn-HTPhC** and **Mn-WTPHC** determined by ICP-MS were  $6.6 \times 10^{-4}$  and  $3.4 \times 10^{-4}$   $\mu$ mol, respectively, in the buffer solution. The suspended solution was exposed to the LED light at 456 nm. The spectra were recorded at 5 min intervals, and corrected at 550 nm to determine the conversions of deoxy-Mb to MbCO by using calculations reported previously.<sup>25,42</sup> The experiments were performed in triplicate and the data represent mean  $\pm$  SEM.

suggested by the IR spectrum of **Mn-HTPhC** and the  $\text{Mn}(\text{CO})_3\text{Br}(\text{bpy})$  complex (Fig. 2b).<sup>43</sup> The IR spectrum of **Mn-HTPhC** after the Mb assay with light irradiation indicates complete release of CO from **Mn-HTPhC** due to the absence of bands assignable to CO stretching (Fig. 2b, dotted line). The half-life ( $t_{1/2}$ ) of CO release from **Mn-HTPhC** was found to be  $5.7 \pm 0.3$  min with light irradiation. The value is comparable to that of photoCORM immobilized in non-woven and polymer (Table S2, ESI†).<sup>10,44</sup> The number of Mn ions per PhM retained in **Mn-HTPhC** after the Mb assay is  $5.8 \pm 1.0$ . This value is similar to the number of Mn ions determined before initiation of the assay ( $5.6 \pm 1.2$ ). These results suggest that Mn ions are retained in **Mn-HTPhC** after CO release. The amount of released CO per Mn of **Mn-WTPHC** with light irradiation is  $1.9 \pm 0.1$  with a  $t_{1/2}$  value of  $6.9 \pm 0.1$  min. These results suggest that His-tag fragments of HTPHC contribute to acceleration of CO release in greater amounts and with a sharper response than WTPHC. Quantum yields of the precursor complex, **Mn-HTPhC** and **Mn-WTPHC** are 0.23, 0.047, and 0.013, respectively.

**Mn-HTPhC** was employed as an ECM for photoactivatable CO release to evaluate the activity of NF- $\kappa$ B by CO gas stress.<sup>45,46</sup> When **Mn-HTPhCs** suspension was added to each well, most of **Mn-HTPhCs** interacted with the cell surface (Fig. S4, ESI†).<sup>33</sup> The cell viability test assessed by the MTT assay indicates no cytotoxicity of **Mn-HTPhC** as well as other composites except for  $\text{Mn}(\text{CO})_5\text{Br}$  under light irradiation (Fig. 4a). Since it is well known that the amount and the rate of CO induction into living cells are essential for the activation of NF- $\kappa$ B,<sup>47</sup> the activity of NF- $\kappa$ B is expected to be controlled by **Mn-HTPhC** in the presence or the absence of light irradiation.<sup>48</sup> The activity of  $\kappa$ B-Fluc transfected HEK293 cells (HEK293/ $\kappa$ B-Fluc) cultured with **Mn-HTPhC** and TNF- $\alpha$  was assessed by examining the bioluminescence intensity of HEK293 cells after 12 hours incubation (Fig. 4b). **Mn-HTPhC** showed the activation of

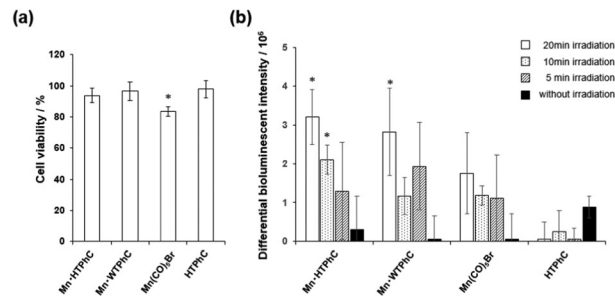


**Fig. 4** Evaluation of **Mn-HTPhC** as a CORM-ECM for cell viability (a), and NF- $\kappa$ B activity (b). Each sample was incubated with HEK293/ $\kappa$ B-Fluc cells under 5%  $\text{CO}_2$  at 37  $^\circ\text{C}$ . The viability was evaluated by examining cell populations after incubation for 12 hours after light irradiation for 20 min. Luminescence intensity in the luciferase reporter assay for the evaluation of NF- $\kappa$ B activity of HEK293/ $\kappa$ B-Fluc cells in the presence of 10 ng  $\text{mL}^{-1}$  TNF- $\alpha$  after incubation for 12 hours with **Mn-HTPhC**, **Mn-WTPHC**,  $\text{Mn}(\text{CO})_5\text{Br}$  and HTPHC, with the light irradiation for 20 min (white), 10 min (dot), 5 min (slashed) and without the light irradiation (black). \* $P < 0.05$  vs. PBS buffer for a and b, respectively. Each experiment was performed in triplicate and the data represent mean  $\pm$  SEM.

NF- $\kappa$ B almost comparable to **Mn-WTPHC** under light irradiation for 20 min. Only **Mn-HTPhC** had a significant activation of NF- $\kappa$ B with 10 min light irradiation. There were no significant differences among the composites with 5 min light irradiation or in the dark. The activation of NF- $\kappa$ B by **Mn-HTPhC** with 10 min light irradiation is expected to be caused by *ca.* 1.5-fold larger amount of CO from **Mn-HTPhC** than that of **Mn-WTPHC** (Fig. 3b), although **Mn-HTPhC** and **Mn-WTPHC** shows only slight difference on half-lives.<sup>35</sup>  $\text{Mn}(\text{CO})_5\text{Br}$  showed less significant effect on the NF- $\kappa$ B activation. This result could be due to cytotoxicity of free Mn species after the CO release with the light irradiation because the complex did not show the toxicity before light irradiation (Fig. 4a and Fig. S5, ESI†). Thus, these results indicate that **Mn-HTPhC** can safely release CO to activate NF- $\kappa$ B by suppressing the cytotoxicity of the  $\text{Mn}(\text{CO})$  moieties in the crystals.

In conclusion, light-triggered CO-releasing ECMs were constructed by immobilizing  $\text{Mn}(\text{CO})$  moieties in PhCs. When a His-tag fragment is fused to the C-terminus of PhM, the resulting composite HTPHC gains the ability to accumulate twice the number of Mn moieties relative to the unmodified WTPHC. Moreover, **Mn-HTPhC** releases a stoichiometric amount of CO molecules per Mn ion. The release effectively contributes to activation of NF- $\kappa$ B by suppressing the cytotoxicity of the precursor complex,  $\text{Mn}(\text{CO})_5\text{Br}$ . These results suggest that photoactivatable CO release from engineered protein crystals will be adaptable to provide information regarding cellular events involving CO gas. Since CO release is expected to be regulated at a specific time point during the course of cellular proliferation, we are investigating the detailed mechanisms of CO biology using these composites.

The authors thank Prof. S. Kizaka-Kondoh and Dr T. Kuchimaru, and Dr H. Ohtani (Tokyo Institute of Technology, Japan) for their discussions. Parts of this work were supported by the Funding Program for Next-Generation World-Leading Researchers



(grant number LR019 for T. U.) for Scientific Research on Innovative Areas (26102513 for T. U. and 15K07794 for H. M.) from Ministry of Education, Culture, Sports, Science and Technology, and Research Fellowship for Young Scientists (for H. T.) from the Japan Society for the Promotion of Science.

## References

- 1 R. Motterlini and L. E. Otterbein, *Nat. Rev. Drug Discovery*, 2010, **9**, 728–743.
- 2 T. R. Johnson, B. E. Mann, J. E. Clark, R. Foresti, C. J. Green and R. Motterlini, *Angew. Chem., Int. Ed.*, 2003, **42**, 3722–3729.
- 3 B. E. Mann and R. Motterlini, *Chem. Commun.*, 2007, 4197–4208.
- 4 M. Kajimura, R. Fukuda, R. M. Bateman, T. Yamamoto and M. Suematsu, *Antioxid. Redox Signaling*, 2010, **13**, 157–192.
- 5 U. Schatzschneider, *Br. J. Pharmacol.*, 2015, **172**, 1638–1650.
- 6 J. E. Clark, P. Naughton, S. Shurey, C. J. Green, T. R. Johnson, B. E. Mann, R. Foresti and R. Motterlini, *Circ. Res.*, 2003, **93**, E2–E8.
- 7 U. Hasegawa, A. J. van der Vlies, E. Simeoni, C. Wandrey and J. A. Hubbell, *J. Am. Chem. Soc.*, 2010, **132**, 18273–18280.
- 8 H. Yin, J. Fang, L. Liao, H. Nakamura and H. Maeda, *J. Controlled Release*, 2014, **187**, 14–21.
- 9 P. Peng, C. Wang, Z. Shi, V. K. Johns, L. Ma, J. Oyer, A. Copik, R. Igarashi and Y. Liao, *Org. Biomol. Chem.*, 2013, **11**, 6671–6674.
- 10 P. C. Kunz, H. Meyer, J. Barthel, S. Sollazzo, A. M. Schmidt and C. Janiak, *Chem. Commun.*, 2013, **49**, 4896–4898.
- 11 G. Doerdelmann, H. Pfeiffer, A. Birkner and U. Schatzschneider, *Inorg. Chem.*, 2011, **50**, 4362–4367.
- 12 G. Doerdelmann, T. Meinhardt, T. Sowik, A. Krueger and U. Schatzschneider, *Chem. Commun.*, 2012, **48**, 11528–11530.
- 13 A. E. Pierri, P.-J. Huang, J. V. Garcia, J. G. Stanfill, M. Chui, G. Wu, N. Zheng and P. C. Ford, *Chem. Commun.*, 2015, **51**, 2072–2075.
- 14 U. Schatzschneider, *Inorg. Chim. Acta*, 2011, **374**, 19–23.
- 15 R. D. Rimmer, A. E. Pierri and P. C. Ford, *Coord. Chem. Rev.*, 2012, **256**, 1509–1519.
- 16 M. A. Gonzales and P. K. Mascharak, *J. Inorg. Biochem.*, 2014, **133**, 127–135.
- 17 J. Niesel, A. Pinto, H. W. P. N'Dongo, K. Merz, I. Ott, R. Gust and U. Schatzschneider, *Chem. Commun.*, 2008, 1798–1800.
- 18 P. C. Kunz, W. Huber, A. Rojas, U. Schatzschneider and B. Spingler, *Eur. J. Inorg. Chem.*, 2009, 5358–5366.
- 19 M. A. Gonzalez, M. A. Yim, S. Cheng, A. Moyes, A. J. Hobbs and P. K. Mascharak, *Inorg. Chem.*, 2012, **51**, 601–608.
- 20 R. Kretschmer, G. Gessner, H. Gorls, S. H. Heinemann and M. Westerhausen, *J. Inorg. Biochem.*, 2011, **105**, 6–9.
- 21 A. J. Atkin, I. J. S. Fairlamb, J. S. Ward and J. M. Lynam, *Organometallics*, 2012, **31**, 5894–5902.
- 22 C. S. Jackson, S. Schmitt, Q. P. Dou and J. J. Kodanko, *Inorg. Chem.*, 2011, **50**, 5336–5338.
- 23 C. Bischof, T. Joshi, A. Dimri, L. Spiccia and U. Schatzschneider, *Inorg. Chem.*, 2013, **52**, 9297–9308.
- 24 A. E. Pierri, A. Pallaoro, G. Wu and P. C. Ford, *J. Am. Chem. Soc.*, 2012, **134**, 18197–18200.
- 25 R. Motterlini, J. E. Clark, R. Foresti, P. Sarathchandra, B. E. Mann and C. J. Green, *Circ. Res.*, 2002, **90**, E17–E24.
- 26 M. A. Gonzales, H. Han, A. Moyes, A. Radinos, A. J. Hobbs, N. Coombs, S. R. J. Oliver and P. K. Mascharak, *J. Mater. Chem. B*, 2014, **2**, 2107–2113.
- 27 S. Garcia-Gallego and G. J. L. Bernardes, *Angew. Chem., Int. Ed.*, 2014, **53**, 9712–9721.
- 28 S. H. Heinemann, T. Hoshi, M. Westerhausen and A. Schiller, *Chem. Commun.*, 2014, **50**, 3644–3660.
- 29 H. Inaba, K. Fujita and T. Ueno, *Biomater. Sci.*, 2015, **3**, 1423–1438.
- 30 N. E. Bruckmann, M. Wahl, G. J. Reiss, M. Kohns, W. Watjen and P. C. Kunz, *Eur. J. Inorg. Chem.*, 2011, 4571–4577.
- 31 I. S. Albuquerque, H. F. Jeremias, M. Chaves-Ferreira, D. Matak-Vinkovic, O. Boutureira, C. C. Romao and G. J. L. Bernardes, *Chem. Commun.*, 2015, **51**, 3993–3996.
- 32 M. Chaves-Ferreira, I. S. Albuquerque, D. Matak-Vinkovic, A. C. Coelho, S. M. Carvalho, L. M. Saraiva, C. C. Romao and G. J. L. Bernardes, *Angew. Chem., Int. Ed.*, 2015, **54**, 1172–1175.
- 33 H. Tabe, K. Fujita, S. Abe, M. Tsujimoto, T. Kuchimaru, S. Kizaka-Kondoh, M. Takano, S. Kitagawa and T. Ueno, *Inorg. Chem.*, 2015, **54**, 215–220.
- 34 H. Tabe, T. Shimoi, K. Fujita, S. Abe, H. Ijiri, M. Tsujimoto, T. Kuchimaru, S. Kizaka-Kondo, H. Mori, S. Kitagawa and T. Ueno, *Chem. Lett.*, 2015, **44**, 342–344.
- 35 K. Fujita, Y. Tanaka, T. Sho, S. Ozeki, S. Abe, T. Hikage, T. Kuchimaru, S. Kizaka-Kondoh and T. Ueno, *J. Am. Chem. Soc.*, 2014, **136**, 16902–16908.
- 36 K. Fujita, Y. Tanaka, S. Abe and T. Ueno, *Angew. Chem., Int. Ed.*, 2015, **55**, 1056–1060.
- 37 H. Inaba, N. J. M. Sanghamitra, K. Fujita, T. Sho, T. Kuchimaru, S. Kitagawa, S. Kizaka-Kondoh and T. Ueno, *Mol. Biosyst.*, 2015, **11**, 3111–3118.
- 38 S. Abe and T. Ueno, *RSC Adv.*, 2015, **5**, 21366–21375.
- 39 F. Coulbaly, E. Chiu, K. Ikeda, S. Gutmann, P. W. Haebe, C. Schulze-Bries, H. Mori and P. Metcalf, *Nature*, 2007, **446**, 97–101.
- 40 H. Ijiri, F. Coulbaly, G. Nishimura, D. Nakai, E. Chiu, C. Takenaka, K. Ikeda, H. Nakazawa, N. Hamada, E. Kotani, P. Metcalf, S. Kawamata and H. Mori, *Biomaterials*, 2009, **30**, 4297–4308.
- 41 M. Razavet, V. Artero, C. Cavazza, Y. Oudart, C. Lebrun, J. C. Fontecilla-Camps and M. Fontecave, *Chem. Commun.*, 2007, 2805–2807.
- 42 A. J. Atkin, J. M. Lynam, B. E. Moulton, P. Sawle, R. Motterlini, N. M. Boyle, M. T. Pryce and I. J. Fairlamb, *Dalton Trans.*, 2011, **40**, 5755–5761.
- 43 P. Govender, S. Pai, U. Schatzschneider and G. S. Smith, *Inorg. Chem.*, 2013, **52**, 5470–5478.
- 44 C. Bohlender, S. Gläser, M. Klein, J. Weissner, S. Thein, U. Neugebauer, J. Popp, R. Wyrwa and A. Schiller, *J. Mater. Chem. B*, 2014, **2**, 1454–1463.
- 45 H. S. Kim, P. A. Loughran, P. K. Kim, T. R. Billiar and B. S. Zuckerbraun, *Biochem. Biophys. Res. Commun.*, 2006, **344**, 1172–1178.
- 46 H. S. Kim, P. A. Loughran, J. Rao, T. R. Billiar and B. S. Zuckerbraun, *Am. J. Physiol.: Gastrointest. Liver Physiol.*, 2008, **295**, G146–G152.
- 47 S. Chlopicki, M. Lomnicka, A. Fedorowicz, E. Grochal, K. Kramkowski, A. Mogielnicki, W. Buczek and R. Motterlini, *Naunyn-Schmiedeberg's Arch. Pharmacol.*, 2012, **385**, 641–650.
- 48 A. R. Brasier, J. E. Tate and J. F. Habener, *Biotechniques*, 1989, **7**, 1116–1122.

